Experimental model of a hydrogen fuel cell using graphene pads as heat spreaders

Álvaro García-Martínez[a], Aitor Fernández-Jiménez[b], Eduardo Álvarez-Álvarez[c], Eduardo Blanco-Marigorta[d] and María José Suárez-López[e]

[a] Departamento de Energía, Universidad de Oviedo, C/Wifredo Ricart s/n, Gijón, Asturias (España), 33203, garciaalvaro@uniovi.es
[b] fernandezaitor@uniovi.es,
[c] edualvarez@uniovi.es
[d] eblanco@uniovi.es
[e] suarezlmaria@uniovi.es

Abstract:

The implementation of new low-carbon technologies for electricity generation and storage will involve the use of new resources such as hydrogen. In this sense, the use of hydrogen fuel cells will make it possible to store and transport energy for subsequent use by industry or other consumption. However, these devices generate large amounts of heat, which reduces their electrical efficiency. For this reason, recent studies have focused on the use of carbon allotropes, such as graphene, as heat sinks. This work presents a reduced model of a hydrogen fuel cell with graphene sheets, which has been subjected to several experimental tests, varying its heating and cooling conditions. Thus, the main objective of the experiment was to find out how the graphene sheets behave under different heat gradients and to assess their suitability as a heat sink. Specifically, temperature values, gradients and heat maps have been obtained in the different cells that make up the experimental prototype. In this way, the high performance of graphene as a heat sink in hydrogen fuel cells has been confirmed.

Keywords:

Heat dissipation; graphene; hydrogen fuel cells; experimental test rig.

1. Introduction

Hydrogen, the most abundant chemical element in nature, is a low-carbon resource whose only emission when burned is water vapour. This inert gas has been used in industry since the beginning of the 20th century and today, thanks to the stabilisation of its volatility, it has begun to be used in the automotive and aerospace industries [1]. The main advantage of this fuel is that it does not emit polluting gases to atmosphere. It is this last characteristic that has recently attracted increasing interest. In fact, the World Hydrogen Council (WHC) estimates that by 2030 the energy generated by the use of this green fuel will reach 3000 TWh/year [2].

Hydrogen energy is stored using electrochemical devices called fuel cells, where chemical energy is converted directly into electricity. The fuel (hydrogen) and comburent (oxygen) undergo a chemical exchange to produce water and electricity in the form of direct current and heat [3]. There are several types of hydrogen fuel cells, depending on the type of electrolyte used, which determines the type of chemical reactions that take place in the cell (see Table 1).

Table 1. Classification of hydrogen cells according to electrolyte type [3].

Fuel cell	Proton Exchange Membrane Fuel Cell (PEMFC)	Phosphoric Acid Fuel Cell (PAFC)	Molten Carbonate Fuel Cell (MCFC)	Solid Oxide Fuel Cell (SOFC)
Electrolyte	Solid polymer	Phosphoric acid	Molten carbonates	Solid polymer
Operating temperature (ºC)	60 – 80	200 – 250	600 – 700	50 – 120
Power range (kW)	5 – 250	5 – 150	100 – 2000	5
Advantages	Low temperature	Accept impure H_2	Cogeneration	No fuel reforming required
Applications	Transport	Electricity generation	Electricity generation	Electricity generation
Efficiency	34%	38%	48%	47%

https://doi.org/10.52202/069564-0093

These devices have among their characteristics the need to operate in an optimum temperature range to achieve high performance and minimise their degradation [4]. Specifically, the most common ways of removing excess heat inside hydrogen cells are free convection, condensers, heat sinks and cooling plates [5]. Heat dissipation by convection is therefore the simplest system, since all that is done is to add fins to the cell interfaces and leave them in contact with air, so it is only feasible at low temperatures [6]. Dissipation by condensers or cooling plates involves much more complex designs and the incorporation of devices that force the movement of a fluid (water or air) to force this dissipation, so they are used in batteries with high temperature ranges [7]. Finally, the use of heatsinks is based on the concept of thermal conductivity to transport heat to a cold source (passive or active). This implies the use of different materials that have adequate thermal conductivity behaviour (K in W/mK) [8].

In the specific case of heatsinks, the material from which they are made is particularly important, as it will transfer heat more or less efficiently depending on its thermal conductivity. In addition, other properties such as anisotropy, size, aspect ratio or the orientation of its atomic structure are key to ensuring proper heat exchange [9]. Up to now, the main materials used to dissipate heat in hydrogen fuel cells have been steel, aluminium and copper, the latter being the most suitable but also the most expensive [10]. However, the use of new polymers and carbon-derived materials (allotropes) is taking over much of the research into heat dissipation in hydrogen fuel cells.

The most important compound of carbon allotropes is graphene, since it is the basic element from which other materials such as graphite, fullerenes or carbon nanotubes (CNTs) are obtained. On the one hand, the main properties of these compounds are a well-defined atomic structure [11], high thermal conductivity (≈ 2000 W/mK), low coefficient of thermal expansion, strong mechanical and chemical resistance and anisotropy [12]. On the other hand, they have the disadvantage of being technically difficult to produce, and their high price undermines their competitiveness compared to other common materials. In fact, these materials have only been studied using advanced numerical models and, after sintering in the laboratory, they have been thermally characterised [13].

For example, in the research by Bahru et al…, a study is carried out using different techniques to characterise graphene, determining some thermal parameters according to the manufacturing method used (thickness, K or thermal resistance) for its subsequent use as a heat dissipating material in fuel cells [14]. In addition, the paper by Sun et al. carried out a numerical simulation of the heat transfer phenomena that occur in high-power LED light emitters, complementing the study with experimental tests based on thermography [11]. Finally, the article by Suzsko et al. presents a numerical analysis of the anisotropy of graphene for its use as a dissipator in high-efficiency microprocessors and its comparison with other materials [15].

In this sense, the present paper carries out an experimental study on the use of graphene sheets for heat dissipation inside a hydrogen fuel cell. For this purpose, a reduced scale model of a hydrogen fuel cell has been designed and fabricated, which has been subjected to a series of experimental tests simulating the heat exchange processes that occur during the operation of the cell. In each of the tests, temperature, gradient and heat map values were obtained to study the behaviour of graphene as a heat spreader.

2. Materials and methods

2.1. Experimental model

To study the thermal conductivity of graphene as a heat spreader, a reduced model of a hydrogen cell was designed, manufactured and studied in different experimental tests. In addition, to know its behaviour under different operating conditions, three different cases were simulated: Case 1, 2 and 3 (see Figure 1). In cases 1 and 2, passive cooling is used since the fins (case 1) and the graphene solid (case 2) are in exclusive contact with air. In case 3, however, both the fins and the graphene solid are in direct contact with a liquid cooling unit (active cooling).

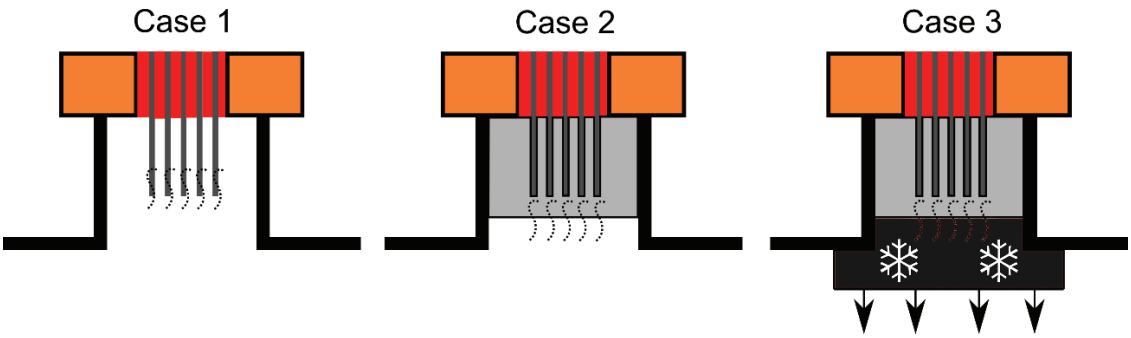

Figure 1. Geometry of the different cases implemented.

In all three cases, the functional scheme of the experimental model was the same. Specifically, the battery is made up of 5 identical cells placed one after the other. Each cell contains a heating pad with a maximum power of 5 W and a size of 100x50 mm, powered by a DC power supply. This makes it possible to control the operating temperature range of the system. This pad is flanked on both sides by a thermal interface with a conductivity of 3 W/mK to ensure heat transfer between cells. In turn, between two successive cells, a 0.5 mm thick graphene sheet measuring 120x50 mm has been placed to channel the heat flow towards some external fins where the cooling (passive or active) will take place. Finally, the whole system is supported by a 20 mm thick wooden case and a clamping system that ensures suitable contact between all the layers. Figure 2 shows a photograph of the implemented scale model and the location of the temperature sensors in each layer.

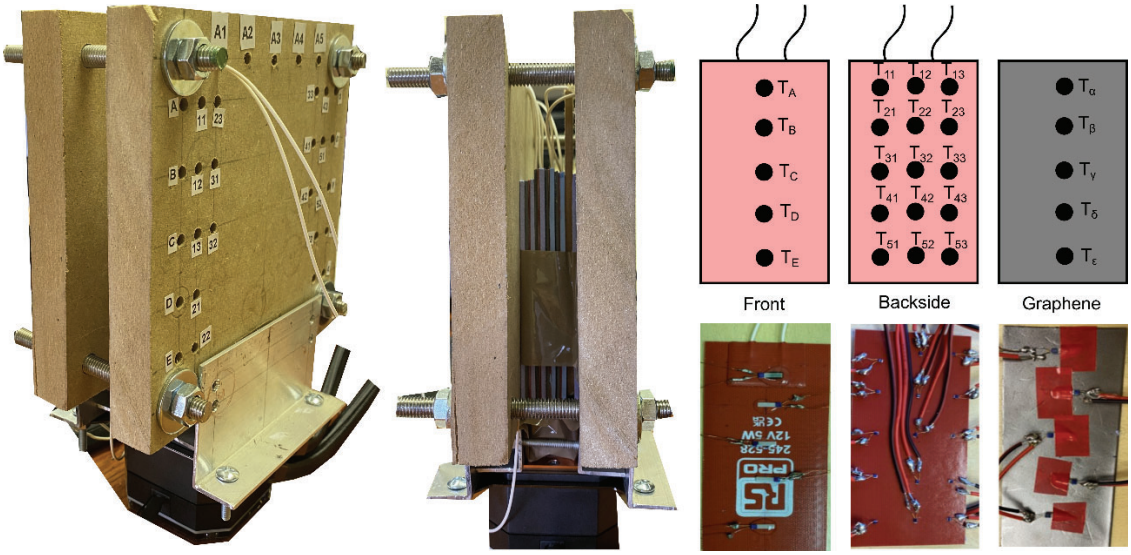

Figure 2. Photograph of the reduced experimental model and location of temperature sensors on each sheet of the fuel cell.

The parameter used for the study was temperature, using resistance thermometers according to the required accuracy of measurement. These sensors were only placed in the central cell of the reduced model because it was considered that this is the section where the greatest amount of heat is generated and therefore the study will be more interesting. Thus, as shown in Figure 3, fifteen temperature sensors were placed in an array on the back (T_{ij} ... $T_{(i+4,j+2)}$) and five temperature sensors on the front (T_A ... T_E) of the heating pad. In this way, the first ones make it possible to obtain a map of the heat distribution over the entire surface where the heat is generated, while the second ones were placed along the centre line to obtain the temperature gradient in the heating pad. In addition, five temperature sensors were placed along the axis of the graphene sheet (T_α ... T_ϵ) and one additional temperature sensor in the lamellar area (T_{flap}). In this way it was possible to obtain the temperature gradients in the carbon allotrope. Finally, it should be noted that several temperature sensors resistors were also used to obtain the temperature in other parts of the model: the contact zone between the graphene and the cooling unit (T_{con}), and two to obtain the ambient temperature on the surface of the case (T_m) and in the room (T_{amb}).

The temperature data are recorded using a data acquisition unit (model DAQ970A) for subsequent analysis. In addition, the cooling unit used (model iCUE H150i ProXT) can be controlled by computer, allowing the heat dissipation of the experimental model to be varied. All the tests were carried out in the maximum heat extraction mode. The experimental test rig used is shown in the following photograph (see Figure 3).

https://doi.org/10.52202/069564-0093

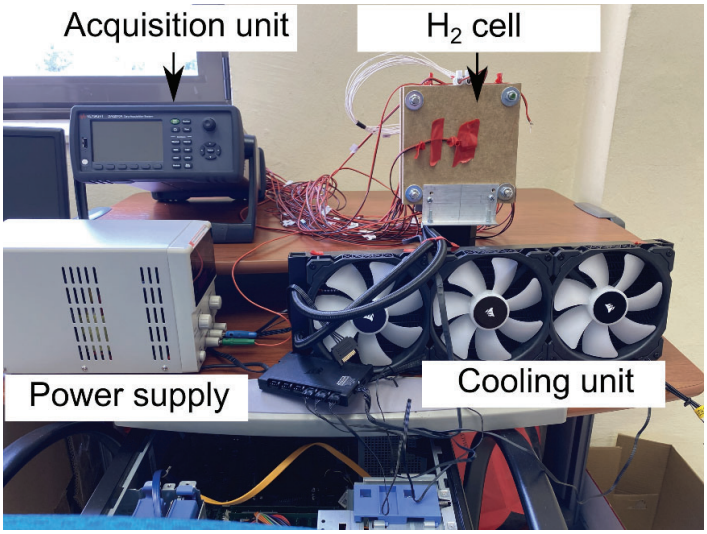

Figure 3. Experimental test rig designed and used for experimental tests.

To minimise the influence of external effects on the experiment, a constant temperature of 23°C was maintained in the room through the use of an air-conditioning unit. In addition, the prototype has been protected from solar radiation due to the use of opaque curtains that prevent the penetration of the sun's rays into the interior of the room. Finally, it should be noted that the effect of artificial convection was not considered relevant during the tests, since the air-conditioning unit kept the temperature values constant.

3. Results and analysis

For each of the cases implemented, tests were carried out focusing on the behaviour of the graphene sheet, while at the same time confirming the correct functioning of the heating pad. In this way, it was possible to obtain the temperature variation over time, the temperature gradient along the central part of the graphene sheet and the thermal maps in both materials.

The test consisted of switching on each of the heating pads with a power of 1 W, producing a heating phase of the stack for 40 minutes. This simulates the heat that would be generated inside the battery during operation. After this time, the power supply is switched off and the cooling phase begins. In cases 1 and 2 the cooling was passive (natural convection), while in case 3 the cooling unit remained on throughout the test (heating-cooling phases). The tests were repeated twice, obtaining consistent and reproducible results.

In case 1, the curves of the temperature variation with time during the whole duration of the test and the variation of the temperature gradient along the length of the sheet at the moment t = 40 min were obtained (see Figure 4).

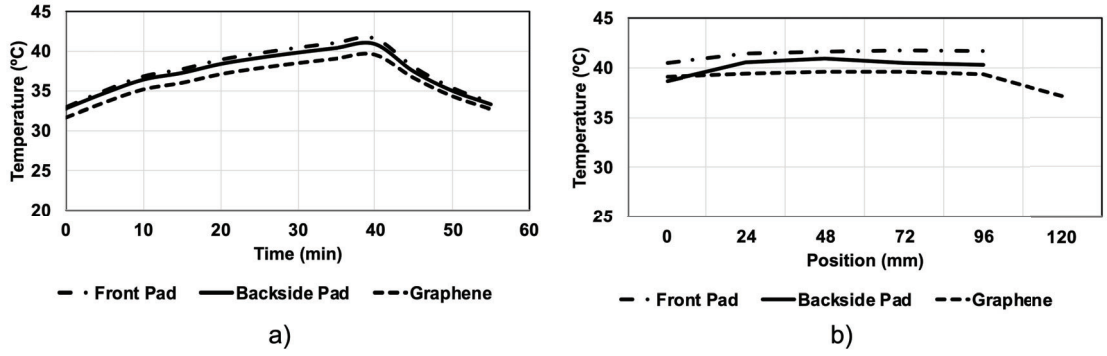

Figure 4. a) Temperature variation throughout the test and b) temperature gradient along the central section of the pad and graphene at t=40 min. Case 1.

For case 2, the same curves have also been obtained (see Figure 5).

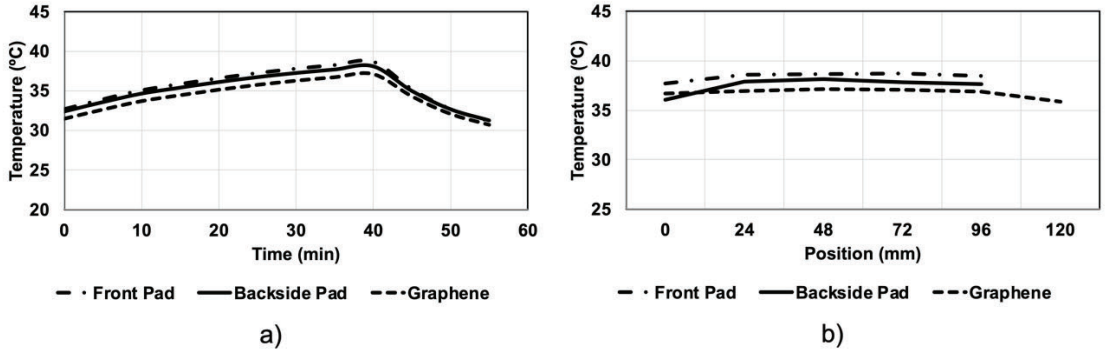

Figure 5. a) Temperature variation along the whole test and b) temperature gradient along the central part of the pad and graphene at t=40 min. Case 2.

Finally, Figure 6 shows the same graphs as above but for case 3.

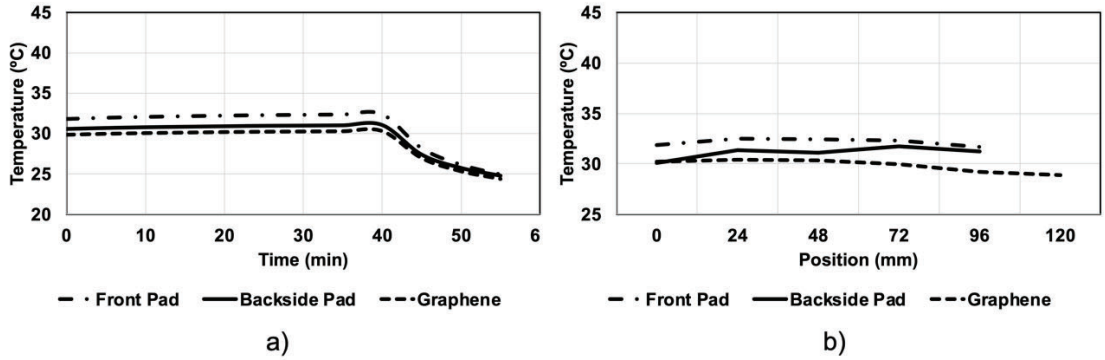

Figure 6. a) Temperature variation during the test and b) temperature gradient along the middle part of the pad and graphene at t=40 min. Case 3.

Note that in all cases both the back and the inside of the pad reach a higher temperature than the graphene sheet, which corresponds to reality as it is the heat source. Furthermore, looking at the temperature gradients, the pad still reaches a higher temperature than the graphene. It should be noted that the line representing the graphene sheet reaches up to 120 mm, since this position corresponds to the fins or the contact with the cooling unit, depending on the case considered. These results confirm that the equipment worked correctly in the three experimental cases considered. In addition, Figure 7 shows the heat maps obtained in the back of the heating pad in cases 1, 2 and 3.

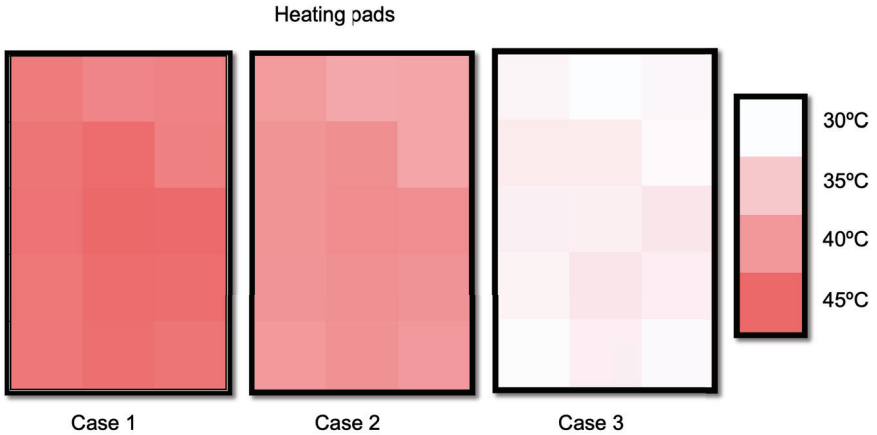

Figure 7. Heat maps for all three cases on the backside of the heating pad.

https://doi.org/10.52202/069564-0093

It can be seen that, in all cases, the temperature differences are less than 275,15 ºK, so it can be considered that the entire surface of the heating pad has a homogeneous behavior, confirming its correct functioning. Focusing on the graphene sheet, Figure 8 shows a comparison of the three experimentally studied cases.

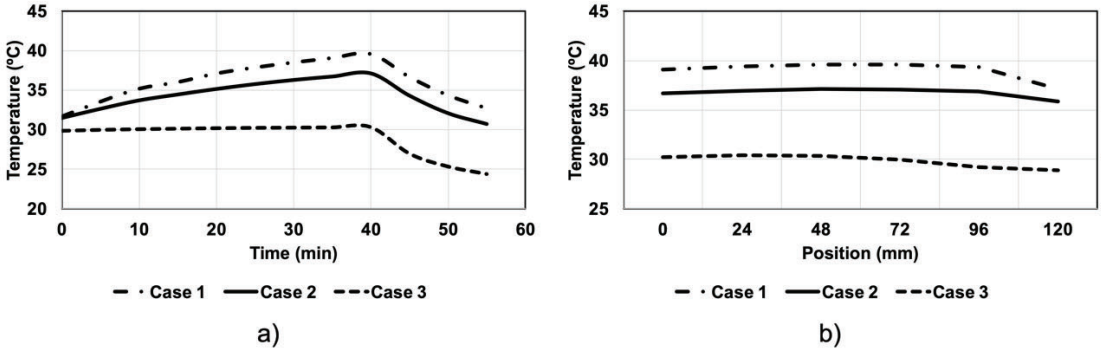

Figure 8. Comparison between the three cases considered: a) temperature variation in the graphene during the test and b) temperature gradient along the graphene sheet at t=40 min.

On the one hand, looking at Figure 8a, we can see that in the passive cooling cases, the graphene gradually increases its temperature until, at t=40 min, it abruptly starts its cooling phase. However, in case 3, since the cooling unit is on throughout the test, we can see how the graphene maintains a constant temperature during the heating phase, thanks to its thermal homogeneity properties. Then, from t=40 min, its temperature drops abruptly as the cooling unit actively removes the heat.

On the other hand, in Figure 8b, the temperature gradients in the central part of the graphene sheet show a negative slope to the left, i.e. the heat extraction is at the 120 mm position. Moreover, this slope is weak due to the latent isotropy in the graphene, which acts as a suitable heat sink.

4. Conclusions

The development of new low-carbon technologies for electricity generation and the construction of devices that allow more effective energy storage will be key to addressing future energy scenarios. In this sense, hydrogen-based technology will play a fundamental role through the development and implementation of batteries that allow safe and effective energy storage. However, these devices generate large amounts of heat, which significantly reduces their efficiency. To improve the efficiency of these devices, carbon allotropes such as graphene have recently been used. One of the many properties of these materials is their high thermal conductivity, which makes them ideal for use as heat sinks. Recent research has been based on the in-depth characterisation of this new material from a technical point of view, achieving in some cases conductivity values close to 6000 W/mK.

This publication shows an investigation through the construction of a reduced hydrogen cell model to study how graphene works as a heat sink in these devices. Specifically, three different cases were carried out in which the cooling conditions (passive and active) were varied. In this way, the aim is to verify that graphene can be used as a thermal conductor, allowing optimal heat extraction inside hydrogen cells. To this end, the temperature variation at different points of a graphene sheet under heating and cooling conditions was studied. In addition, the temperature gradients and their variation with the position in the material sheet itself have been calculated by studying the thermal slopes. In both cases, it has been confirmed that the heat dissipation takes place towards the location of the fins and the cooling unit, thus presenting a suitable thermal homogeneity.

In particular, graphene performs very well as a heat spreader, with temperature differences of less than 2ºC achieved along the entire length of the sheet. Moreover, when the same graphene surfaces are used to dissipate heat to the outside (cases 1 and 2), the temperature does not increase by more than 15ºC with respect to the ambient temperature. Finally, if a sufficiently powerful active cooling unit is used, the temperatures inside the cell are only 3ºC higher than the ambient temperature.

From the results obtained, it was found that the high thermal conductivity of the graphene allows efficient heat extraction to the cooling points. In addition, the graphene sheet has a very homogeneous behaviour, so that its entire surface reaches practically the same temperature, which translates into efficient heat transport.

Future work will validate a numerical model based on CFD, which will allow the simulation of passive and active cooling conditions, so that it will be possible to vary the heat extraction scenarios. It will also be possible to test other materials used as heat sinks, such as aluminium or copper. It is also planned to repeat the experimental tests but with different materials and compare the results with those presented in this article.

Acknowledgments

This work was carried out in the framework of Next Generation Heat Sink Design Project (Reference AYUD/2021/57485), funded by Principality of Asturias through FICYT and co-funded by ERDF. Also, the authors would like to thank the company The Next Pangea for their participation and collaboration.

References

[1] S. P. Yu *et al.*, "Integration of low-pressure hydrogen storage cylinder and automatic controller for carbon deposit removal in car engine," *Int J Hydrogen Energy*, vol. 41, no. 46, pp. 21795–21801, Dec. 2016, doi: 10.1016/J.IJHYDENE.2016.07.191.

[2] IEA, "The Future of Hydrogen – Analysis - IEA," 2021. https://www.iea.org/reports/the-future-of-hydrogen (accessed Mar. 09, 2021).

[3] S. Mekhilef, R. Saidur, and A. Safari, "Comparative study of different fuel cell technologies," *Renewable and Sustainable Energy Reviews*, vol. 16, no. 1, pp. 981–989, Jan. 2012, doi: 10.1016/J.RSER.2011.09.020.

[4] R. A. Felseghi, E. Carcadea, M. S. Raboaca, C. N. Trufin, and C. Filote, "Hydrogen Fuel Cell Technology for the Sustainable Future of Stationary Applications," *Energies 2019, Vol. 12, Page 4593*, vol. 12, no. 23, p. 4593, Dec. 2019, doi: 10.3390/EN12234593.

[5] "Fuel Cell Heat Management." https://www.fuelcellstore.com/blog-section/fuel-cell-heat-transfer-management (accessed Feb. 23, 2023).

[6] M. D. Mat and K. Aldas, "Application of a two-phase flow model for natural convection in an electrochemical cell," *Int J Hydrogen Energy*, vol. 30, no. 4, pp. 411–420, Mar. 2005, doi: 10.1016/J.IJHYDENE.2004.04.002.

[7] J. Choi, Y.-H. Kim, Y. Lee, K.-J. Lee, and Y. Kim, "Mechanical Science and Technology Numerical analysis on the performance of cooling plates in a PEFC," *Journal of Mechanical Science and Technology*, vol. 22, pp. 1417–1425, 2008, doi: 10.1007/s12206-008-0409-6.

[8] D. Hu, J. Liu, F. Yi, Q. Yang, and J. Zhou, "Enhancing heat dissipation to improve efficiency of two-stage electric air compressor for fuel cell vehicle," *Energy Convers Manag*, vol. 251, p. 115007, Jan. 2022, doi: 10.1016/J.ENCONMAN.2021.115007.

[9] L. Fan, Z. Tu, and S. H. Chan, "Recent development of hydrogen and fuel cell technologies: A review," *Energy Reports*, vol. 7, pp. 8421–8446, Nov. 2021, doi: 10.1016/J.EGYR.2021.08.003.

[10] L. Vasiliev and L. Vassiliev Jr, "Heat Pipes in Fuel Cell Technology," *Proceedings of the NATO Advanced Study Institute on Mini-Micro Fuel Cells-Fundamental and applications*, 2007. https://www.researchgate.net/publication/271074215_Heat_Pipes_in_Fuel_Cell_Technology (accessed Feb. 23, 2023).

[11] Q. Sun, J. Liu, Y. Peng, A. Wang, Z. Wu, and M. Chen, "Effective heat dissipation of high-power LEDs through creation of three-dimensional ceramic substrate with kaolin/graphene suspension," *J Alloys Compd*, vol. 817, p. 152779, Mar. 2020, doi: 10.1016/J.JALLCOM.2019.152779.

[12] A. A. Balandin, "Thermal Properties of Graphene, Carbon Nanotubes and Nanostructured Carbon Materials," California, US: National Library of Medicine, 2011.

[13] Y. Zhang *et al.*, "Recent advanced thermal interfacial materials: A review of conducting mechanisms and parameters of carbon materials," *Carbon N Y*, vol. 142, pp. 445–460, Feb. 2019, doi: 10.1016/J.CARBON.2018.10.077.

[14] R. Bahru *et al.*, "Allotrope carbon materials in thermal interface materials and fuel cell applications: A review," *Int J Energy Res*, vol. 44, no. 4, pp. 2471–2498, Mar. 2020, doi: 10.1002/ER.5077.

[15] A. Suszko and M. S. El-Genk, "Thermally anisotropic composite heat spreaders for enhanced thermal management of high-performance microprocessors," *International Journal of Thermal Sciences*, vol. 100, pp. 213–228, Feb. 2016, doi: 10.1016/J.IJTHERMALSCI.2015.09.018.

 https://doi.org/10.52202/069564-0093